

## 6.2. CORRELATION OF RADIOCARBON AND VARVE CHRONOLOGIES OF LAKE GOŚCIAŻ

Tomasz Goslar, Anna Pazdur, Mieczysław F. Pazdur†, Maurice Arnold & Irena Hajdas

### Bulk samples

The 35 samples covering the whole profile were chosen for radiocarbon dating (see Goslar, Chapter 4.2.1) in the Gliwice Radiocarbon Laboratory. The carbonate and organic fractions were dated separately. Application of the conventional radiocarbon dating method to dating lake sediments is difficult because initial  $^{14}\text{C}$  activity of sediment is as a rule unknown and may differ from corresponding value of the contemporary biosphere. The main reason for the difference is that total dissolved inorganic carbon (DIC) in the lake water incorporates undetermined amounts of carbon from different reservoirs, with concentration of  $^{14}\text{C}$  ranging from 0 to 100 pmc (percent modern carbon). Moreover, the sedimentation of lake marl is influenced in different ways by the presence of water plankton and vascular water plants. The main sources of organic carbon in lake sediment are lacustrine phytoplankton, lacustrine macrophytes, and terrestrial plants (Pearson & Coplen 1978). The initial  $^{14}\text{C}$  activity in lacustrine organisms may be as low as it is in DIC; however, admixture of terrestrial plants causes the  $^{14}\text{C}$  activity of the organic fraction to be usually higher than that of contemporaneous carbonate sediment. Both fractions in modern samples may reveal an apparent age ranging up to a few thousands of years. The dates of bulk samples have been already published (Pazdur et al. 1987a, b, 1995) in comparison with earlier versions of the varve chronology. They confirmed approximately the annual character of laminations, at least within the limit of reasonable variation of the apparent age. Here (Fig. 6.3) we compare the  $^{14}\text{C}$  dates with the recent version of the varve chronology.

The apparent age of the organic fraction varies between 300 and 2000 years, being the lowest at ca. 11.2 kyr BP, i.e. after the climatic warming at the onset of the Holocene. In the Holocene, two periods may be distinguished: an earlier one of lower apparent age and a later one of higher age. This seems to correspond to the long-term changes of sediment composition, i.e. the proportion between the organic and carbonate fractions, determined along the whole profile by loss on ignition (LOI) at 550°C and 900°C (Wicik 1993). In the lower panel of Fig. 6.3 the apparent age of the organic fraction of bulk samples is compared with that calculated with a very simple model, in which two sources of DIC in the lake are considered:  $^{14}\text{C}$  depleted bicarbonate ions coming with the groundwater, and  $\text{CO}_2$  exchanged with the atmosphere. The basic assumption of this model is that in a non-productive lake the proportion between both fluxes

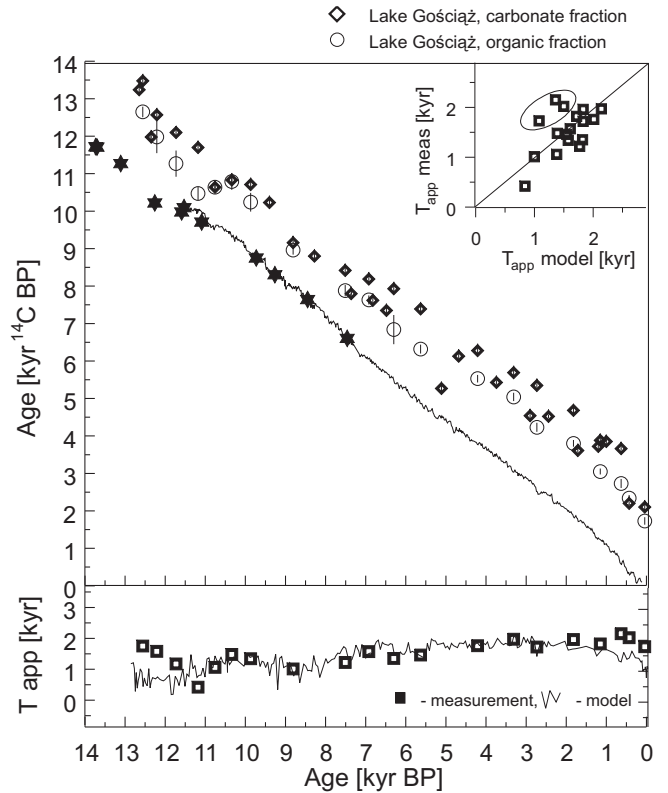


**Fig. 6.3.** Comparison of radiocarbon ages of carbonate and organic fraction of bulk samples of sediment from Lake Gościąg with radiocarbon calibration based on wood dated dendrochronologically (curve) and on corals dated by the U/Th method (stars). Lower part: comparison of measured apparent ages of organic fraction of bulk samples and that derived from the model described in the text. Upper-right panel: Correlation between measured and model-calculated apparent ages of samples from Holocene section of sediment. The youngest three samples have been enclosed by an ellipse.

remains constant. This proportion is disturbed by photosynthesis of lacustrine plants, which diminishes the pressure of dissolved carbon dioxide and causes an additional flux of  $\text{CO}_2$  from the atmosphere, which balances the increased deposition of carbon. The specific activity of  $^{14}\text{C}$  in DIC would then be equal to:

$$A_{DIC} = (A_{np} \cdot F_{np} + A_{atm} \cdot F_{bio}) / (F_{np} + F_{bio})$$

where  $F_{np}$  and  $F_{bio}$  denote the net flux of carbon to a non-productive lake and additional flux caused by lacustrine plants, and  $A_{np}$  and  $A_{atm}$  are the specific activities of  $^{14}\text{C}$  in non-productive lakes and in the atmosphere. The apparent age can then be calculated as:

$$T_{app} = -8033 \cdot \ln (A_{DIC}/A_{atm}) = -8033 \cdot \ln \left[ \frac{A_{np} + F_{bio}/F_{np}}{A_{atm} + F_{bio}/F_{np}} \right]$$

Assuming constant ratio of radiocarbon activity in the inflowing water and in atmosphere, the variations of apparent age in the model are only the function of ratio of additional to "normal" net fluxes of carbon. The ratio of both fluxes can be approximated by the proportion of carbon deposited in organic and inorganic form, which

may be reconstructed using known contents of organic and carbonate fraction. Here, it has been adopted that:

$$\frac{F_{bio}}{F_{np}} = 4 \cdot \frac{LOI}{CaCO_3}$$

The coefficient 4 is the approximate ratio of carbon content in the organic fraction (ca. 50%) and in calcium carbonate (12%). The ratio between organic carbon and LOI is determined by comparison with direct measurements of organic carbon content (Łacka et al., Chapters 7.3 and 8.2). As the radiocarbon activity of inflowing water, the mean value of the measurements in modern groundwater (68 pmc, Kuc, pers. comm.) was used.

The agreement between apparent ages calculated by the given formula and those measured in the Holocene section of sediment (upper-right part of Fig. 6.3) is quite good ( $r = 0.56$ ). The correlation is much better when the youngest three samples are excluded ( $r = 0.86$ ). These samples have an apparent age higher than predicted by the model. It should be noted that in the youngest 600 yr of the profile the ratio of organic carbon to LOI is distinctly lower than 0.5.

One must stress that the approach presented here is highly simplified, since it assumes that the proportion between fluxes of  $^{14}\text{C}$  depleted and “modern” carbon is altered only by organic productivity, the depletion of  $^{14}\text{C}$  in groundwater is constant, the radiocarbon in forming the organic matter is in equilibrium with that in DIC, and the input of terrestrial organics to the sediment is negligible. It also does not explain the variations of apparent age of the carbonate fraction. A quite different approach, using the variations of apparent age of carbonate fraction to reconstruct the relative changes of lake’s depth was recently published by Pazdur et al. (1995). The approach presented here does not pretend to be applied as a “real” model. It was rather used to demonstrate that the observed large variations of apparent age along the profile of sediment are reasonable, and that one cannot expect an accurate verification of varve chronology using the radiocarbon dates of bulk samples. Much more precise radiocarbon dating of lacustrine sediment is possible when the macrofossils of terrestrial plants are used.

### Terrestrial macrofossils

Since the introduction of AMS technique for radiocarbon dating, the short-living parts of land plants have been frequently used for dating lake sediments (Andree et al. 1986, Hajdas et al. 1993). The age of such samples is free of hard-water (or reservoir) effects. A danger of dating rebedded macrofossils still exists and cannot be avoided entirely. However, in the case of laminated sediments, the redeposition within the lake is usually limited to such events as turbidites and slumps. For a given plant fragment, the delay between its growth and deposition in the

lake is usually not known, but it seems negligible if the dates of a number of samples are consistent. Some problems arise from the small mass of samples: in the typical AMS facility, the precision of  $^{14}\text{C}$  measurement falls distinctly when the sample mass declines below 1 mg. In the sediment of Lake Gościąg terrestrial macrofossils occur very rarely, and the samples in the first set were usually smaller than 1 mg. For the second set, in order to gather samples large enough, the macrofossils were collected from several precisely correlated cores (G1/87, G2/87, G1/90, G2/91, T1/90) and, besides the short-living macrofossils widely used in dating of lake sediment (birch nutlets, birch fruit scales, pine bud scales, willow leaves), the fragments of pine peridermis were collected (Tab. 6.2). Peridermis is formed directly under the bark of a tree stem or twig and should have the same  $^{14}\text{C}$  activity as contemporaneous short-living parts of tree. One could expect that deposition of dead peridermis is delayed more than for other types of macrofossils. This was checked by separate dating of pine peridermis and bud scales found in the same varves, and the results are compared in Fig. 6.4. Though the dates of paired scales (S) and peridermis (P) agree within the precision of dating ( $\chi^2 = 2.99$ ;  $df = 5$ ), the P samples are usually older than S. However, the comparison of mean age difference between P and S –  $75 \pm 68$  yr does not indicate that the ages of both types of samples are significantly discordant.

Another problem connected with the small mass of sample is the danger of contamination. It has been shown (Wohlfarth et al. 1993) that contamination may alter the age of macrofossils by even a few thousands of years. According to Wohlfarth (pers. comm.) the process responsible for the contamination is the assimilation of modern carbon by fungi growing on macrofossils during

**Table 6.2.** List of types of terrestrial plant macrofossils, used for AMS dating of the Lake Gościąg sediments. The plants and types of macrofossils are ordered according to their abundance.

| Plant name                       | Type of macrofossils   |
|----------------------------------|--|
| 1. <i>Pinus sylvestris</i> L.    | peridermis,<br>bud scales,<br>needles,<br>peridermis with bark,<br>bark, seeds with wing,<br>seeds |
| 2. <i>Betula</i> sp.             | nutlets with wing,<br>female catkin scales,<br>nutlets without wing                                |
| 3. <i>Salix</i> sp.              | leaf fragments,<br>peridermis  |
| 4. <i>Alnus</i> sp. <sup>1</sup> | nutlets,<br>fructification fragments   |
| 5. <i>Tilia</i> sp. <sup>1</sup> | anthers  |

<sup>1</sup> – only in the Holocene section of sediment.

**Table 6.3.** AMS radiocarbon dates of terrestrial macrofossils from a fragment of annually laminated sediments of Lake Gościąg. The varves are numbered in continuous sequence, from the oldest to the youngest, and zero varve corresponds to the sandy layer. The YD/PB boundary corresponds to the varve no. 1072. The calendar age ( $\pm 120$ yr) is given according to the match to German oak chronology.

S, P – samples of pine scales and peridermis from the same horizon. 1 – samples of scales and peridermis from section of irregular lamination in core T1/90, not dated by varve chronology, 2 – sample probably contaminated with modern carbon, 3 – sample dated in ETH Zürich. Other samples were dated in Gif-sur-Yvette.

| Sample code | Mass mgC | Varve no.   | Age cal BP | Age C14 BP      | Comment        |
|-------------|----------|-------------|------------|-----------------|----------------|
| 93 319      | 0.97     | 1 475+1 535 | 11 010     | 9 600 $\pm$ 90  | S              |
| 93 320      | 2.60     | 1 475+1 535 | 11 010     | 9 650 $\pm$ 110 | P              |
| 93 332      | 1.67     |             | ca. 10 430 | 9 340 $\pm$ 120 | S <sup>1</sup> |
| 93 335      | 1.74     |             | ca. 10 430 | 9 480 $\pm$ 120 | P <sup>1</sup> |
| 93 416      | 0.57     |             | ca. 10 330 | 9 050 $\pm$ 130 | S <sup>1</sup> |
| 93 417      | 1.74     |             | ca. 10 330 | 8 980 $\pm$ 100 | P <sup>1</sup> |
| 93 310      | 0.57     | 1 595+1 655 | 10 890     | 9 560 $\pm$ 90  | S              |
| 93 331      | 0.66     | 1 595+1 655 | 10 890     | 9 770 $\pm$ 120 | P              |
| 93 338      | 2.77     | 1 765+1 805 | 10 730     | 9 430 $\pm$ 100 | P              |
| 93 337      | 0.77     | 1 765+1 805 | 10 730     | 9 400 $\pm$ 100 | S              |
| 93 382      | 0.90     | 2 530+2 630 | 9 935      | 9 030 $\pm$ 90  |                |
| 93 355      | 0.77     | 2 575+2 705 | 9 875      | 8 610 $\pm$ 100 |                |
| 93 383      | 0.90     | 2 625+2 665 | 9 870      | 9 000 $\pm$ 90  |                |
| 93 384      | 0.91     | 2 665+2 705 | 9 830      | 8 850 $\pm$ 90  |                |
| 93 328      | 0.91     | 2 775+2 815 | 9 720      | 8 650 $\pm$ 100 |                |
| 93 314      | 1.20     | 2 805+2 845 | 9 690      | 8 920 $\pm$ 90  |                |
| 93 390      | 1.62     | 2 865+2 885 | 9 640      | 8 950 $\pm$ 70  |                |
| 93 356      | 1.06     | 2 885+2 935 | 9 605      | 8 560 $\pm$ 80  |                |
| 93 358      | 2.48     | 3 005+3 065 | 9 480      | 8 280 $\pm$ 90  | 2              |
| 93 359      | 1.02     | 3 115+3 185 | 9 365      | 8 340 $\pm$ 80  |                |
| 93 330      | 0.93     | 3 305+3 325 | 9 200      | 8 280 $\pm$ 100 |                |
| 93 329      | 0.46     | 3 355+3 385 | 9 145      | 8 140 $\pm$ 110 |                |
| 93 360      | 0.99     | 3 665+3 785 | 8 790      | 7 930 $\pm$ 90  |                |
| 93 313      | 1.23     | 3 860+3 890 | 8 640      | 8 010 $\pm$ 80  |                |
| 93 361      | 0.94     | 3 945+4 015 | 8 535      | 7 910 $\pm$ 90  |                |
| 93 362      | 0.88     | 4 055+4 115 | 8 430      | 7 600 $\pm$ 100 |                |
| 93 368      | 0.84     | 4 290+4 330 | 8 205      | 7 280 $\pm$ 100 |                |
| 1MZ+2MZ     |          | 3 567+3 742 | 8 858      | 7 740 $\pm$ 85  | 3              |
| 7MZ         |          | 4 102+4 187 | 8 368      | 7 740 $\pm$ 70  | 3              |
| 9MZ         |          | 4 667+4 787 | 7 785      | 7 075 $\pm$ 80  | 3              |
| 11+12MZ     |          | 6 432+6 592 | 6 000      | 5 505 $\pm$ 90  | 3              |
| 14MZ        |          | 7 537+7 627 | 4 930      | 4 255 $\pm$ 70  | 3              |

their storage between coring and target preparation. In order to minimize the contamination, we used only large, well preserved fragments, and after each step of preparation they were rinsed with large amount of distilled water and closed tightly in a small vial with a drop of water. Moreover, the outer surface of plant fragments was scraped with the soft plastic brush, once during identification and once again directly prior to the first stage of AAA pretreatment. Each mechanical contact with the sample was controlled under binocular microscope. The good agreement of the obtained dates with the radiocarbon calibration data proves that the contamination of Lake Gościąg macrofossils is, as a rule, negligible.

The radiocarbon dates of terrestrial macrofossils of Lake Gościąg have been used for the absolute dating of the floating varve chronology (FVC) and for reconstructing the variations of atmospheric <sup>14</sup>C activity at the Late-Glacial/early-Holocene transition (Goslar et al., Chapter 7.7). Here, only the results concerning the dating of FVC are discussed. Five dates have been obtained in Eidgenössische Technische Hochschule, Zürich (Hajdas et al. 1995), the other ones come from the Centre des Faibles Radioactivites, Gif-sur-Yvette, France. They are listed in Tab. 6.3 and presented on the background of radiocarbon calibration data in Fig. 6.5. Since the differences of calendar ages of samples are known, the absolute age can

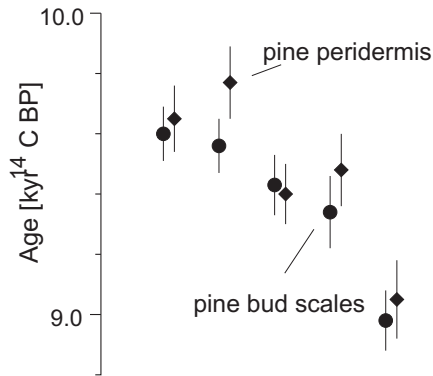


**Fig. 6.4.** Comparison of AMS radiocarbon ages of pine bud scales and pine peridermis samples from laminated sediments of Lake Gościąż. For each of 5 pairs, both samples were collected from the same varves.

be determined by means of the wiggle-matching procedure (see Pearson 1986). In this procedure, the age of the floating varve chronology (FVC) giving minimum mean-square difference between radiocarbon dates of macrofossils and those derived from  $^{14}\text{C}$  calibration curve was sought. Since the errors of radiocarbon dates differ from one another, the original procedure was slightly modified by calculating the sum of square differences of dates weighed by their errors, i.e.:

$$S_m^2(T_{FVC}) = \frac{1}{n} \sum_{i=1}^n \frac{(x_i - y(T_{FVC} + T_i))^2}{(\sigma_{x_i}^2 + \sigma_y^2(T_{FVC} + T_i))}$$

where  $T_{FVC}$  and  $T_i$  denote the calendar age of younger end of FVC and the age of  $i$ -th sample with respect to younger end of FVC,  $x_i$ ,  $\sigma_{x_i}$  denote the radiocarbon date of  $i$ -th sample and its error, and  $y_i$ ,  $\sigma_y$  are the corresponding ages derived from the  $^{14}\text{C}$  calibration curve by linear interpolation between data points. The adopted manner for determining  $y_i$  and  $\sigma_y$  differs slightly from that applied by Kruse et al. (1980) and Pearson (1986), who used the smoothed version of calibration curve. Of course, since the position of each sample with respect to FVC ( $T_i$ ) is known, the values of  $y_i$  and  $\sigma_y$  depend only on the calendar age of FVC,  $T_{FVC}$ . The expected value of S-square statistics is 1, and its confidence intervals can be derived from the chi-square distribution. As the calibration data, we used those published by Stuiver & Becker (1993), Pearson et al. (1993) and Kromer & Becker (1993). Because the dendrochronological dating of the pine chronology covering the early part of Holocene is still tentative (Kromer & Becker 1993), the samples from that period were not included in the calculations.

To collect enough material for AMS dating, the macrofossils for some samples were collected from sections comprising more than 150 varves. The uncertainty of sample position with respect to varve chronology was then significant when compared to errors of AMS dating. It has been taken into account by the definition of  $S_m^2$ :

$$S_m^2(T_{FVC}) = \frac{1}{n} \sum_{i=1}^n \frac{(x_i - y(T_{FVC} + T_i))^2}{(\sigma_{x_i}^2 + \sigma_{T_i}^2 + \sigma_{y_i}^2(T_{FVC} + T_i))}$$

where  $\sigma_{T_i}$  denotes the error of sample position (i.e. the half-thickness of section). It must be mentioned that such an approach is correct only if the slope of the calibration curve is  $45^\circ$ . This is not exactly the case, and the statistical weight of each date should depend also on the shape of the calibration curve around the calendar age  $T_{FVC} + T_i$ . The development of a more adequate procedure will be the matter for further study.

The function  $S_m^2(T_{FVC})$  has very fine structure, which seems insignificant because of the unknown shape of the calibration curve between data points and because of the uncertainty of sample position  $T_i$ , so in Fig. 6.6a the smoothed functions were plotted. The mean square difference for all 13 dates obtained at Gif has a broad minimum for the age of FVC between 3170 cal BP and 3020 cal BP. However, the function  $S_m^2(T_{FVC})$  depends strongly on the date of one critical sample, placed at the steep slope of calibration curve (at ca. 9.6 kyr BP). The minimum of  $S_m^2$  calculated after rejection of the critical date is distinctly wider, i.e. between 3260 cal BP and 3020 cal BP. The placing of FVC between 3260 cal BP and 3170 cal BP assumes that the critical sample is too young by more than 400 yr. The only reliable explanation of such an effect is a contamination by younger material; as one can note from Tab. 7.4 in Chapter 7.7, the obvious contamination of similar magnitude appeared in the sample from the middle of Younger Dryas (sample no. 93324). The addition of Swiss results does not change the match significantly. The top of FVC can then be dated by the AMS radiocarbon method to  $3140 \pm 120$  cal BP. This age

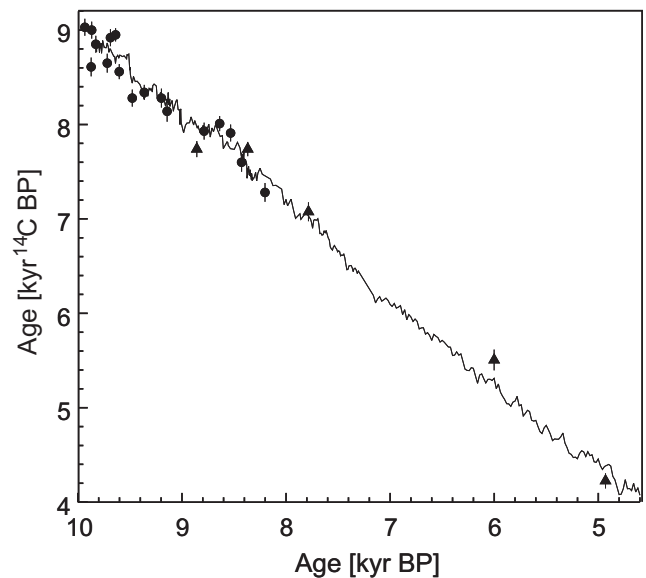


**Fig. 6.5.** The results of AMS radiocarbon datings of terrestrial macrofossils from Lake Gościąż sediments, on the background of radiocarbon calibration curve obtained on German oaks. Triangles – samples dated in Zürich, circles – samples dated in Gif-sur-Yvette.

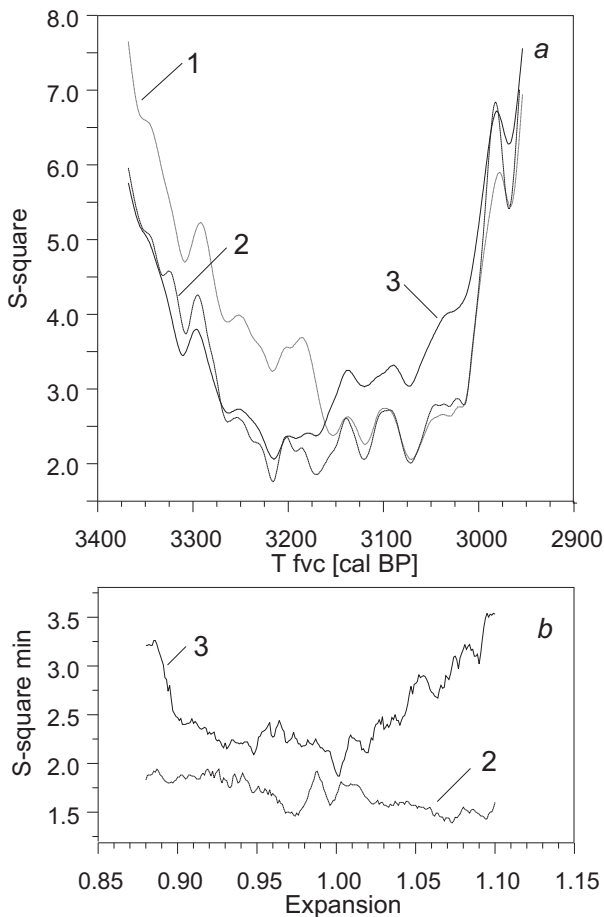


**Fig. 6.6.** The results of wiggle matching of radiocarbon dates of Lake Gościąg macrofossils with the radiocarbon calibration curve obtained on German oaks. a – mean square differences between radiocarbon dates of LG samples and calibration curve as a function of the age of floating varve chronology (FVC): 1 – for all the samples dated in Gif, 2 – for all the samples dated in Gif, except the critical one (see the text), 3 – for all the samples dated in Gif and in Zürich, except the critical one. b – minimum mean square differences between radiocarbon dates of LG samples and calibration curve versus the expansion of calendar chronology of LG sediments with respect to constructed varve chronology. 2, 3 – description same as above.

is older but still agrees within the limit of error with that estimated by varve counting, i. e.  $2900^{+500}_{-200}$  cal BP.

The value of S-square at the broad minimum ( $S^2_{\min} = 1.7\text{--}1.9$ ) is higher than the expected value. This may be due both to the effects of redeposition and to some overestimation of laboratory precision. For example, multiplying of  $^{14}\text{C}$  errors by a factor of 1.3 would reduce the value of  $S^2_{\min}$  to ca. 1. Another cause might be the uncertainty of varve counting. The error of varve counting (ca. 50 years in the Holocene section of FVC), however, is cumulative, and significant errors of varve counting in short fragments, i. e. between adjacent samples, seem unlikely. To check the effect of systematic error in varve counting, the following test has been made: the time spans between samples were changed proportionally to that determined by varve chronology (the calendar time scale of sediment was thus expanded or compressed), by

a factor ranging from  $Ex = 0.88$  to  $Ex = 1.10$ , and the mean-square difference for the best fit ( $S^2_{\min}$ ) was calculated for each value of  $Ex$ . If the varve counting is correct, the minimum of  $S^2_{\min}$  is expected for  $Ex = 1.00$ . The plot of  $S^2_{\min}(Ex)$  (Fig. 6.6b) clearly shows that any proportional expansion of varve chronology does not improve the match distinctly. It is also clear that the Gif dates alone cannot prove the reliability of varve counting in the floating chronology with satisfactory accuracy, probably because the time span between the youngest and oldest samples is too short (ca. 1700 yr). With the Swiss dates included (time span ca. 4800 yr), the function  $S^2_{\min}$  has a distinct broad minimum for the expansion between 0.93 and 1.02, and the absolute minimum for  $Ex = 1.002$  (i.e. for the expansion of varve time scale by only 0.2%). With all the scepticism according to the significance of narrow minimum at  $Ex = 1.002$ , one can state at least that the  $^{14}\text{C}$  dates in the section 4800 years long do not contradict the reliability of varve counting.

### 6.3. RECORD OF LAMINAE THICKNESS OF THE LAKE GOŚCIAŻ SEDIMENTS, AND ITS CORRELATION WITH ABSOLUTELY DATED TREE-RING WIDTH SEQUENCES

*Tomasz Goslar*

#### The record of laminae thickness

Although the varved sediment of Lake Gościąg has the potential of annual resolution of investigations, the majority of results are based on sampling intervals of ca. 50 years. One exception is the parameter of varve thickness which has annual resolution. The thickness of varve has been used by many authors as a parameter of palaeolimnological and paleoclimatic importance. One example is the annually laminated sediment of Lake Van, Turkey (Kempe & Degens 1979). The sequence of varve thickness, consisting mostly of allochthonous material, is interpreted as the record of annual water inflow from the catchment. In other circumstances, the thickness of authigenic varves may be related to precipitation. This was the case of Malo Jezero at the lagoon of the Adriatic (Seibold 1958), where the thickness of the calcareous laminations was inversely correlated with precipitation. Presumably in drier years, greater sunshine allowed greater photosynthesis and the precipitation of more calcite. Another case are the varves deposited during the prairie stage (ca. 3.8–8.0 kyr BP) of Elk Lake, Minnesota (Anderson 1992), which have a dominant eolian component. The variations of varve thickness in this stage have been explained by the changes of zonal winds, suspending and carrying the loess, and, by comparison with the variations of atmospheric radiocarbon concentration, used to dem-